Self-Consistent Orthogonalized-Plane-Wave Energy-Band Study of Silicon

D. J. STUKEL AND R. N. EUWEMA

Aerospace Research Laboratories, Wright-Patterson Air Force Base, Ohio 45433

A first-principles self-consistent orthogonalized-plane-wave energy-band calculation has been performed for silicon using a nonrelativistic formalism and Slater's free-electron exchange approximation. The imaginary part of the dielectric constant valence- and conduction-band densities of states, spin-orbit splittings, deformation energies, effective masses, and the x-ray form factors (Fourier transforms of the electron charge density) have been calculated. The theoretical results are compared with the available experimental data.

I. INTRODUCTION

A LARGE amount of information, both experimental and theoretical, is available concerning the valence- and conduction-band edges of the homopolar semiconductor, Si. Considerably less knowledge exists concerning the energy-band structure of Si away from the band edges. Unfortunately, most of the theoretical work concerning the band structure of Si is empirical (pseudopotential method,[1-3] full-zone $\mathbf{k} \cdot \mathbf{p}$ method,[4] and effective-mass Hamiltonian method[5]) or semiempirical [empirical refined orthogonalized-plane-wave (OPW) method[6-8]]. The validity of the empirical and semiempirical work all depends on having accurate experimental data. Even when accurate data are available, one question always remains. If some parameters are adjusted to make the calculated band structure agree with some "known" features of the experimental band structure, how does one know that other features of the calculated band structure will then agree with the actual band structure?

In order to eliminate questions of this nature, we have undertaken an almost first-principles calculation of the energy-band structure and related optical properties of Si. The only experimental datum which is used in this calculation is the lattice constant. No claim is made that the results of this calculation will explain all experimental data or that our results are superior to those obtained by other workers. The contribution of this paper is twofold: (1) The work shows what can be done from a more nearly first-principles approach, and (2) this work provides experimentalists with an unbiased set of results which may be useful in interpreting experiments. It is satisfying that our first-principles approach does yield results which compare well with experiment and with the results of other workers whose

calculations relied upon the input of a considerable amount of experimental data.

The purpose of this paper is to present the Si band structure and related optical properties such as the effect of pressure on the band structure, spin-orbit splittings, deformation energies, effective masses, valence- and conduction-band densities of states, imaginary part of the dielectric constant (ϵ_2), and the x-ray form factors (the Fourier transform of the electron charge density) based on a first-principles self-consistent OPW calculation. These calculations were performed using the self-consistent OPW (SCOPW) model developed at Aerospace Research Laboratories. These self-consistent programs have been very successful in calculating the energy-band structures of group III-V, II-VI, and IV compounds.[9-14]

In Sec. II, calculational details of the model are discussed. These include a brief description of the SCOPW model, convergence behavior of the Brillouin-zone averaging and of the OPW series, and interpolation of the SCOPW high-symmetry point results throughout the Brillouin zone. The SCOPW results are given, discussed, and compared with experimental and with other theoretical results in Sec. III. Conclusions are presented in Sec. IV.

II. CALCULATIONAL DETAILS

A. SCOPW Calculations

The OPW method of Herring[15] is used to calculate the electron energies. In the SCOPW model,[9,10] the electronic states are divided into tightly bound core states and loosely bound valence states. The core states must have negligible overlap from atom to atom. They are calculated from a spherically symmetrized crystalline potential.

The valence states must be well described by a modi-

[1] D. Brust, Phys. Rev. **134**, A1337 (1964).
[2] E. O. Kane, Phys. Rev. **146**, 558 (1966).
[3] M. L. Cohen and T. K. Bergstresser, Phys. Rev. **141**, 789 (1966).
[4] M. Cardona and F. H. Pollak, Phys. Rev. **142**, 530 (1966).
[5] G. Dresselhaus and M. S. Dresselhaus, Phys. Rev. **160**, 649 (1967).
[6] F. Herman, R. L. Kortum, and C. D. Kuglin, Intern. J. Quantum Chem. **15**, 533 (1967).
[7] F. Herman, R. L. Kortum, C. D. Kuglin, and R. A. Short, J. Phys. Soc. Japan **21**, 7 (1966).
[8] F. Herman, R. L. Kortum, C. D. Kuglin, and R. A. Short, in *Quantum Theory of Atoms, Molecules and the Solid State*, edited by P. O. Lowdin (Academic Press Inc., New York, 1966), p. 381.

[9] R. N. Euwema, T. C. Collins, D. G. Shankland, and J. S. DeWitt, Phys. Rev. **162**, 710 (1967).
[10] D. J. Stukel, R. N. Euwema, T. C. Collins, F. Herman, and R. L. Kortum, Phys. Rev. **179**, 740 (1969).
[11] D. J. Stukel and R. N. Euwema, Phys. Rev. **186**, 754 (1969).
[12] D. J. Stukel and R. N. Euwema, Phys. Rev. (to be published).
[13] D. J. Stukel, R. N. Euwema, T. C. Collins, and V. Smith, Phys. Rev. B **1**, 779 (1970).
[14] T. C. Collins, D. J. Stukel, and R. N. Euwema, Phys. Rev. B **1**, 724 (1970).
[15] C. Herring, Phys. Rev. **57**, 1169 (1940).

fied Fourier series

$$\psi_{k_0}(r)=\sum_\mu B_\mu\left(\frac{1}{\Omega_0}e^{ik_\mu\cdot r}-\sum_a e^{ik_\mu\cdot R_a}\sum A_{c\mu}{}^a\psi_c(r-R_a)\right),$$

where $k_\mu=k_0+K_\mu$, k_0 locates the electron within the first Brillouin zone, K_μ is a reciprocal-lattice vector, R_a is an atom location, ψ_c is a core wave function, and Ω_0 is the volume of the crystalline unit cell. The coefficients $A_{c\mu}{}^a$ are determined by requiring that $\psi_{k_0}(r)$ be orthogonal to all core-state wave functions. The variation of B_μ to minimize the energy then results in the valence one-electron energies and wave functions.

The dual requirements of no appreciable core overlap and the convergence of the valence wave-function expansion with a reasonable number of OPW's determine the division of the electron states into core and valence states. The $3s$ and $3p$ states of Si are taken as the valence states. The convergence properties of the wave-function expansion are discussed in Sec. II C. The core overlap is less than 0.0008 of an electron.

The calculation is self-consistent in the sense that the core and valence wave functions are calculated alternately until neither changes appreciably. The Coulomb potential due to the valence electrons and the charge density are both spherically symmetrized about each inequivalent atom site. With these valence quantities frozen, new core wave functions are calculated and iterated until the core wave functions are mutually self-consistent. The total electronic charge density is calculated at 650 crystalline mesh points covering 1/24 of the unit cell, and the Fourier transform of $\rho(r)^{1/3}$ is calculated. The new crystal potential is calculated from the old valence charge distribution and the new core

charge distribution. Then new core-valence orthogonality coefficients $A_{c\mu}{}^a$, are calculated. The iteration cycle is completed by the calculation of new valence energies and wave functions. The iteration process is continued until the valence one-electron energies change less than 0.01 eV from iteration to iteration.

The appropriate charge density to use for both the self-consistent potential calculation and the form-factor calculation is the average charge density of all the electrons in the Brillouin zone. In the present self-consistent calculations, this average is approximated by a weighted average over electrons at the Γ, X, L, W, Δ, and Σ high-symmetry points of the Brillouin zone shown in Fig. 1. The weights are taken to be proportional to the volumes within the first Brillouin zone closest to each high-symmetry point. The adequacy of this approximation is discussed in Sec. II B.

The starting crystal potential is represented by a spatial superposition of nonrelativistic self-consistent atomic potentials in the manner of Herman and Skillman.[16] This crystal-potential model (from Herman), which is sometimes called the overlapping free-atomic-potential model, also forms the basis of non-SCOPW band calculations.

One way of taking relativistic effects into account within the framework of nonrelativistic band calculations is with first-order perturbation theory. The perturbing Hamiltonian obtained for the spin-orbit splitting is

$$\hat{H}_{so}=-\tfrac{1}{4}iq^2\hat{\sigma}\cdot[\nabla V(r)\times\nabla],$$

where $V(r)$ is the potential, $\hat{\sigma}$ is the Pauli-spin operator, and q is the fine-structure constant. The $\Gamma_{25'}$ SCOPW-valence wave functions are used in this calculation.

In order to calculate the density of states and the absorptive part of the dielectric constant ϵ_2 a pseudopotential fit is made to the relevant energy levels at the Γ, X, L, W, Δ, and Σ points. The pseudopotential technique is then used to calculate energy differences and transition matrix elements throughout the Brillouin zone.[17] In our experience, this procedure gives the ϵ_2 peaks at the correct energies. However, the relative peak heights do not match experiment because of their dependence upon the poor pseudopotential wave functions, and because of complicated electron-hole and electron-phonon interactions which are ignored in our model.

B. Brillouin-Zone Averaged Charge Density

In determining the valence-electron charge distribution in the SCOPW band calculations, one, in principle, sums the contribution of all occupied valence-band states. In practice, one performs this sum by using a representative sample of points in the reduced zone and
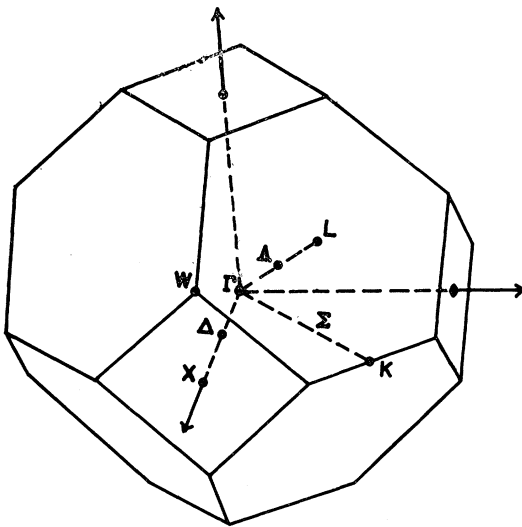
FIG. 1. Zinc-blende Brillouin zone with high-symmetry points labeled. Δ and Σ are symmetries possessed by the Γ-X and Γ-K lines. In our calculations, the midpoint of the lines was used for the Δ point $(\tfrac{1}{2},0,0)$ and Σ point $(\tfrac{1}{2},\tfrac{1}{2},0)$.

[16] F. Herman and S. Skillman, *Atomic Structure Calculations* (Prentice-Hall, Inc., Englewood Cliffs, N.J., 1963).

[17] R. N. Euwema, D. J. Stukel, T. C. Collins, J. S. DeWitt, and D. G. Shankland, Phys. Rev. **178**, 1419 (1969).

assigning suitable weights to the various points. In such calculations, it is also necessary to check the convergence of the solution as a function of the number of points sampled in the reduced zone.

In a previous paper,[10] we presented results based on a one-point, three-point, and four-point sampling. In this paper, we give the results of four-point and six-point sampling. In the four-point sampling (Γ, X, L, and W), the weights used were 0.1258, 0.1731, 0.3600, and 0.3411. For the six-point sampling (Γ, X, L, W, Δ, and Σ), the weights used were 0.03125, 0.09375, 0.125, 0.1875, 0.1875, and 0.375. The weights are proportional to those fractions of the reduced zone which are closer to the point in question than to the remaining points. The six points were selected to provide a uniform sampling of the zone. In Table I, the energy eigenvalues calculated using the four-point sampling are given in column 2 and those obtained using the six-point sampling are given in column 3. The greatest difference in the four- and the six-point eigenvalues is 0.03 eV with the average difference being about 0.01 eV. Hence, the error in the six-point eigenvalues due to the zone sampling is quite small.

In Table II, the theoretical structure factors based on the four-point sampling are given in column 4 and those based on the six-point sampling are given in column 5. The difference in the structure factors due to the number of points sampled is less than 0.01 for all lines except the 222 line, where the difference is 0.03. Hence, one can conclude that the errors introduced by the six-point zone-sampling technique are not significant.

C. OPW Series Convergence

In all OPW band calculations, it is important to make sure that enough OPW terms are included in the vari-

TABLE I. Self-consistent energy eigenvalues for Si based on a four-point (Γ, X, L, and W) and a six-point (Γ, X, L, W, Δ, and Σ) zone sampling. 259 OPW's were used at Γ and a comparable number of OPW's at the other high-symmetry points. The lattice constant used was 5.431 Å. The zero of energy has been placed at the top of the valence band ($\Gamma_{25'}$). All entrees are in eV.

Level	Four-point sampling Slater's exchange	Six-point sampling Slater's exchange	Six-point sampling Kohn-Sham's exchange
Γ_{15c}	2.78	2.79	2.33
$\Gamma_{2'c}$	2.76	2.75	3.31
$\Gamma_{25'v}$	0.0	0.0	0.0
Γ_{1v}	−11.75	−11.74	−12.04
X_{4c}	9.79	9.79	9.87
X_{1c}	1.25	1.28	0.34
X_{4v}	−2.72	−2.72	−3.00
X_{1v}	−7.75	−7.75	−7.83
$X_{1c}-X_{4v}$	3.97	4.00	3.34
L_{3c}	3.81	3.83	3.12
L_{1c}	1.59	1.60	1.39
$L_{3'v}$	−1.18	−1.18	−1.26
L_{1v}	−6.76	−6.75	−7.14
$L_{2'v}$	−9.53	−9.53	−9.63
$L_{3c}-L_{3'v}$	4.99	5.01	4.38
$L_{1c}-L_{3'v}$	2.77	2.78	2.65
W_{2c}	10.80	10.80	10.55
W_{1c}	5.14	5.15	4.82
W_{2c}	4.81	4.83	4.01
W_{2v}	−3.58	−3.57	−4.10
W_{1v}	−7.61	−7.61	−7.64
$W_{2c}-W_{2v}$	8.39	8.40	8.11
Δ_{5c}		5.89	5.66
$\Delta_{2'c}$		3.62	2.81
Δ_{1c}		1.55	0.81
Δ_{5v}		−1.78	−2.00
$\Delta_{2'v}$		−3.58	−3.49
Δ_{1v}		−10.69	−10.94
$\Delta_{1c}-\Delta_{5v}$		3.33	2.81
Σ_{1c}		5.54	5.10
Σ_{4c}		5.02	4.60
Σ_{3c}		2.88	2.27
Σ_{2v}		−1.27	−1.40
Σ_{1v}		−3.45	−3.96
Σ_{3v}		−5.40	−5.47
Σ_{1v}		−9.74	−9.92
$\Sigma_{3c}-\Sigma_{2v}$		4.15	3.67

TABLE II. Experimental and calculated structure factors for Si. RHF values give the results for relativistic Hartree-Fock free-atomic charge densities packed in the crystal lattice. Four-point sampling results involve averaging the charge density in the self-consistent iterations and in the structure-factor calculation over the Γ, X, L, and W points, while six-point results were averaged over the Γ, X, L, W, Δ, and Σ points. Sl stands for Slater's exchange. KSG stands for Kohn-Sham-Gaspar's exchange. Sl-RHF and KSG-RHF give structure factors calculated with an SCOPW-valence charge density and a relativistic free-atomic Hartree-Fock core charge density. Structure-factor units are electrons per crystallographic unit cell.

hkl	Expt	RHF	Four-point sampling Sl	Sl	Six-point sampling KSG	Sl-RHF	KSG-RHF
111	11.12±0.04[a]	10.53	10.89	10.88	10.69	10.86	10.70
220	8.78±0.09[b]	8.71	8.77	8.77	8.64	8.72	8.67
311	8.05±0.07[c]	8.16	8.10	8.11	8.01	8.03	8.05
222	0.22±0.04[a]	0.0	0.22	0.19	0.17	0.19	0.17
400	7.40±0.14[c]	7.51	7.53	7.54	7.44	7.46	7.49
313	7.32±0.12[c]	7.18	7.36	7.34	7.21	7.27	7.26
422	6.72±0.06[c]	6.70	6.92	6.81	6.68	6.71	6.73
333	6.43±0.08[c]	6.44	6.50	6.51	6.38	6.40	6.41
511	6.40±0.08[c]	6.44	6.55	6.55	6.42	6.44	6.45
440	6.04±0.15[c]	6.03	6.17	6.17	6.02	6.05	6.07
444	5.00±0.10[c]	4.97	5.12	5.12	4.96	4.99	5.04

[a] L. D. Jennings (private communication to P. M. Raccah).
[b] M. Hart and A. D. Milne, Acta Cryst. A25, 134 (1969).
[c] H. Hattori, H. Kuriyama, and N. Kato, J. Phys. Soc. Japan 20, 1047 (1965).
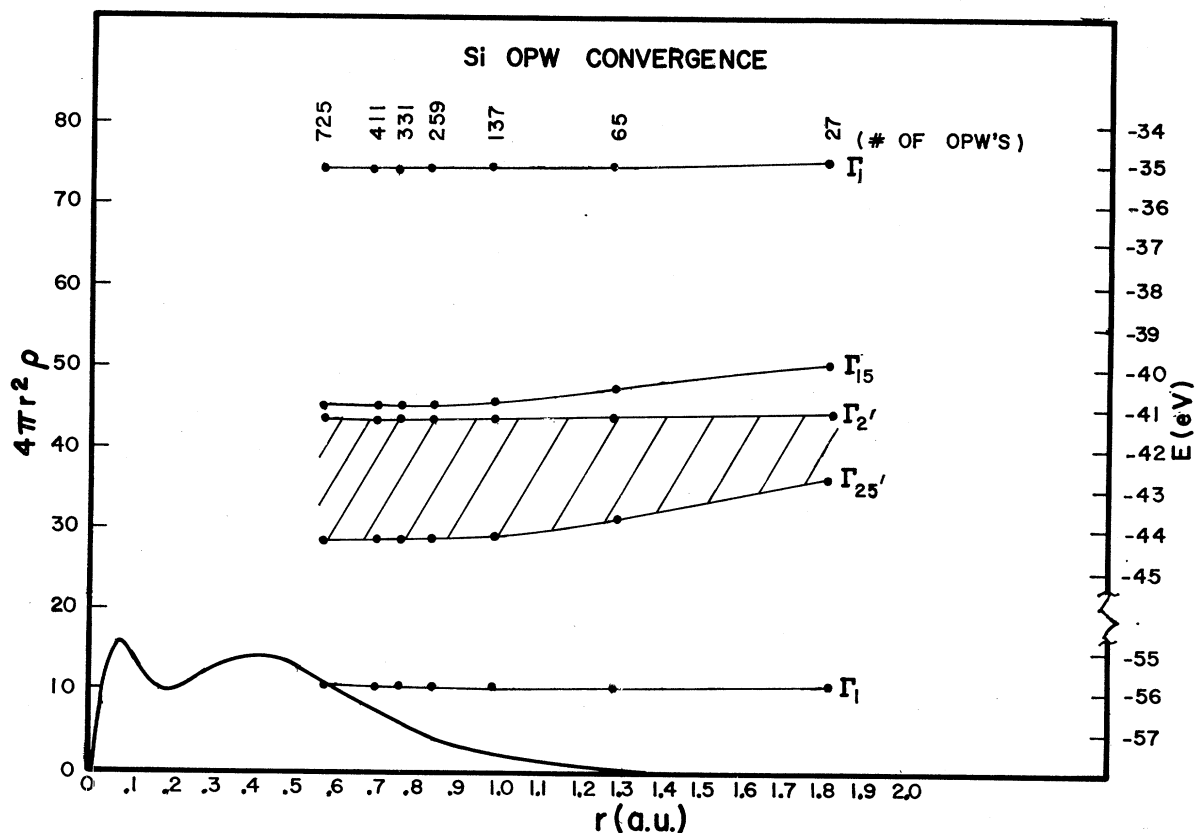
FIG. 2. Convergence study of NSCOPW energy levels at the Γ point in Si.

ational wave functions to ensure a high degree of convergence. The convergence properties of NSCOPW band calculations for Si are illustrated in Fig. 2. In this drawing, the energy levels at Γ are shown as a function of the number of OPW's used and as a function of $\frac{1}{2}\lambda_{min}$. Here, $\lambda_{min} = 2\pi/k_{max}$ where k_{max} is the magnitude of the largest k vector used in the OPW expansion. $\frac{1}{2}\lambda_{min}$ is, thus, the minimum distance that is "felt out" by the plane-wave terms. $4\pi r^2\rho$ is also plotted where ρ is the core density. In order to obtain solutions that are convergent to about 0.02 eV, it is necessary to use about 259 OPW's at the Γ point and a comparable number at the other high-symmetry points. If one increases the number of OPW's at the Γ point from 229 to 259, Γ_{1v}, $\Gamma_{25'v}$ and $\Gamma_{2'c}$ change by less than 0.01 eV and Γ_{15c} changes by less than 0.02 eV. Further increases in the number of OPW's lead to negligible changes in these energy levels. The convergence properties of the energy levels at other high-symmetry points in the zone are similar to those shown in Fig. 2. The convergence properties of the SCOPW band calculations are very similar to those of the NSCOPW band calculations.[18]

---

[18] R. N. Euwema and D. J. Stukel (to be published).

D. Choice of Exchange Potential

In setting up the SCOPW model, one must decide how to handle the exchange and correlation terms. Along with everyone else, we ignore correlation. Since no one has been successful in performing a true Hartree-Fock calculation for a crystal, one of the local exchange approximations must be made. The three most widely used exchange approximations are those of Slater,[19] Kohn and Sham,[20] and Liberman.[21]

The Slater exchange term is given by

$$V_{XS}(r) = -(6/2\pi)k_F(r),$$

where

$$k_F = [3\pi^2\rho(r)]^{1/3},$$

or

$$[E_F - V(r)]^{1/2}.$$

The Kohn and Sham exchange term differs by a factor of $\frac{2}{3}$ from Slater's and is given by

$$V_{XKS}(r) = (-4/2\pi)k_F(r).$$

[19] J. C. Slater, Phys. Rev. 81, 385 (1951).
[20] W. Kohn and L. J. Sham, Phys. Rev. 140, A1133 (1965); R. Gaspar, Acta Phys. Acad. Sci. Hung. 3, 263 (1954).
[21] D. A. Liberman, Phys. Rev. 171, 1 (1968); L. J. Sham and W. Kohn, ibid. 145, 561 (1966).
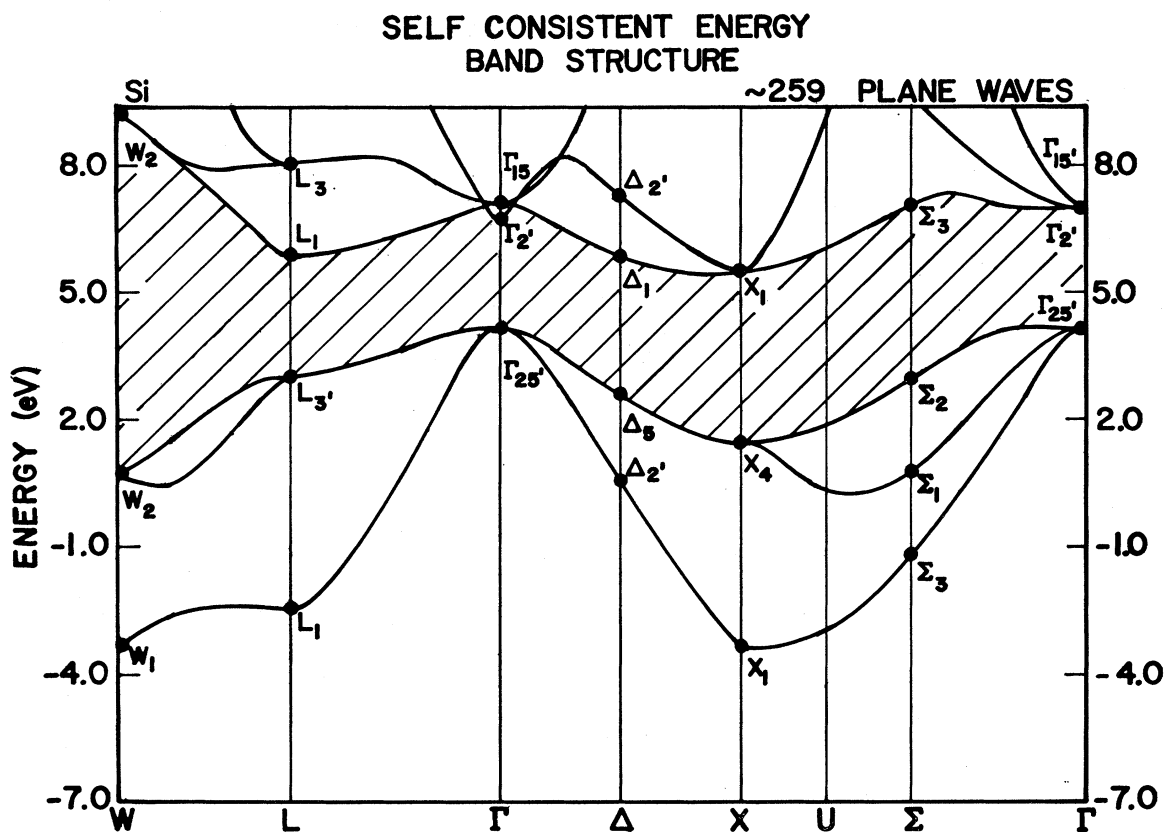
FIG. 3. SCOPW energy-band structure of Si obtained using Slater's exchange. The solid dots denote SCOPW energy levels. The solid lines were obtained by fitting a pseudopotential-type interpolation scheme to the SCOPW energy levels.

Our experience on tetrahedrally bonded semiconductors is that Kohn and Sham's exchange gives bands which are too compressed, while those obtained using Liberman's r-dependent state-dependent exchange are too spread out. The bands obtained using Slater's exchange match experiment very well. Thus, Slater's exchange seems to simulate both exchange and correlation for these crystals.[13]

In Table I, we give the energy eigenvalues obtained using Slater's exchange in column 3 and those obtained using Kohn and Sham's exchange in column 4. The general compression of the bands is indicated by the change of the X_{1c}-X_{4v} from 4.0 eV for Slater's exchange to 3.34 eV for Kohn and Sham's exchange, and the $L_{3c}-L_{3'v}$ from 5.01 eV for Slater's exchange to 4.38 eV for Kohn and Sham's exchange.

III. RESULTS

A. Energy Bands

The SCOPW model contains no adjustable parameters. However, one must supply the lattice constant. In these calculations, the lattice constant used was 5.431 Å determined by Kiendl[22] at 23°C. Self-consistent

calculations were also made with lattice constants of 5.42 and 5.442 Å to calculate the effects of pressure.

The bands obtained using the six-point sampling technique and Slater's exchange are shown in Fig. 3. The eigenvalues are given in column 3 of Table I. These calculations were made using 259 OPW's at the Γ point and a comparable number of OPW's at the other high-symmetry points.

The valence-band structure is very similar to that of other group IV and group III–V compounds. The theoretical SCOPW indirect gap $(\Delta_{1c}{}^m-\Gamma_{25'v})$ is 1.10 eV, and is 0.82 of the distance from the center to the edge of the zone. MacFarlane et al.[23] concluded from their work on the fine structure in the absorption-edge spectrum of Si that the minimum occurred at 0.81 of the distance from the center to the edge of the zone. Experimentally, the indirect gap is 1.13 eV, which is obtained by correcting the gap of 1.115 measured by Frova and Handler[24] by one-third the spin-orbit splitting. The indirect gap is the only key transition whose energy and symmetry are known beyond question.

[22] H. Kiendl. Z. Naturforsch. 22a, 79 (1967).

[23] G. G. MacFarlane, T. P. McLeon, J. E. Quarrington, and V. Roberts, Phys. Rev. 111, 1245 (1958).
[24] A. Frova and P. Handler, Phys. Rev. Letters 14, 178 (1965).

TABLE III. Comparison of theoretical transition energies. Si transition energies derived from different calculations are given in eV. The column headed "present work" gives our unadjusted SCOPW results for Slater's exchange using 259 OPW's. The numbers in parentheses give assumed experimental results which were used in various adjustment procedures.

Transition	Present work	Herman[a]	Kane[b]	Cohen-Bergstresser[c]	Dresselhaus and Dresselhaus[d]
$\Delta_{1c}{}^m - \Gamma_{25'v}$	1.10	1.13(1.13)	1.15(1.15)	0.8(1.1)	1.07(1.1)
$X_{1c} - \Gamma_{25'v}$	1.28	1.3			1.19
$L_{1c} - \Gamma_{25'v}$	1.60	2.25		1.9	1.77
$\Gamma_{15c} - \Gamma_{25'v}$	2.79	2.7	3.2	3.4(3.4)	2.43
$L_{1c} - L_{3'v}$	2.78	3.4(3.4)	2.9	3.1(3.2)	3.20(3.2±0.1)
$\Delta_{1c} - \Delta_{5v}$	3.33	3.4			
$\Gamma_{2'c} - \Gamma_{25'v}$	2.75	4.2	3.3	3.8	3.74(3.75±0.2)
$X_{1c} - X_{4v}$	4.00	4.1	4.1	4.0(4.1)	4.44
$\Sigma_{3c} - \Sigma_{2v}$	4.15	4.3			4.43
$L_{3c} - L_{3'v}$	5.01	4.95	5.3	5.2(5.3)	5.30

[a] References 6 and 8.
[c] Reference 3.
[b] Reference 2.
[d] Reference 5.

Table III gives a comparison of the energy bands obtained from the SCOPW model and those obtained from Herman's[6,8] empirically refined OPW calculation, from Cohen-Bergstresser's[3] and Kane's[2] pseudopotential calculations, and from Dresselhaus and Dresselhaus's effective-mass Hamiltonian calculation.[5] The assumed experimental data which were used in obtaining the various solutions are shown in parentheses in Table III.

Herman calculated the band structure of Si using his empirically adjusted OPW model.[8] In this model, Herman uses the OPW formulation with a potential which is represented by a spatial superposition of overlapping free-atomic potentials. His OPW calculation is not self-consistent. He then uses a three-parameter adjustment scheme to bring the calculated values of three key interband transition energies into agreement with their experimental counterparts (or with his estimate of their experimental counterparts based on his own analysis of experimental reflectivity spectra). Herman[6] indicated that in a three-parameter adjustment scheme he adjusted to $\Delta_{1c}{}^m - \Gamma_{25'v} = 1.13$ eV, $L_{1c} - L_{3'v} = 3.4$ eV (his best estimate at that time), and $\Gamma_{2'c} - \Gamma_{25'v} = 4.05$ eV (the value quoted by Cardona, Shaklee, and Pollak[25] on the basis of their electro-reflectivity measurements). Unfortunately, Herman did not publish in Ref. 6 any detailed solutions for Si. However, Herman[8] did publish detailed solutions for Si based upon a two-parameter adjustment scheme where he adjusted to $\Delta_{1c}{}^m - \Gamma_{25'v} = 1.13$ and $L_{1c} - L_{3'v} = 3.0$, 3.2, and 3.4 eV. The solutions Herman obtained using $L_{1c} - L_{3'v} = 3.4$ eV are quoted in Table III, since this value of $L_{1c} - L_{3'v}$ agrees with his best estimate a year later.

Kane[2] computed the band structure of Si using the Heine-Abarenkov–pseudopotential method. He then adjusted the theoretical Fourier coefficients of the potential on the order of 30% to give agreement with measured cyclotron masses and the indirect gap. Cohen and Bergstresser[3] used the empirical pseudopotential

method to calculate the band structure of Si. Dresselhaus and Dresselhaus[5] developed an effective-mass Hamiltonian in terms of certain Fourier expansion coefficients or band parameters for Si and the resulting energy bands were used to calculate the frequency dependence of the complex dielectric constant. The band parameters were based on 12 optical transitions and cyclotron resonance measurements.

It is clear from Table III that there are wide differences in the theoretical band structures calculated by various authors. Herman and Phillips[26] single out two groups of energy transitions. The "insensitive" transitions do not vary much when the potential is perturbed. They include the $L_{3c} - L_{3'v}$, the $X_{1c} - X_{4v}$, and the $\Gamma_{15c} - \Gamma_{25'v}$. We agree closely with Herman on all these energies. We both disagree with Cohen and Bergstresser on the $\Gamma_{15c} - \Gamma_{25'v}$ transition energy. This is because Cohen and Bergstresser erroneously attributed the 3.4-eV ϵ_2 peak to this transition. The most "sensitive" transitions, according to Herman and Phillips, are the $\Gamma_{2'c} - \Gamma_{25'v}$ and the $L_{1c} - \Gamma_{25'v}$. We differ from Herman by 1.4 eV on the first and by 0.6 eV in the second. Our $\Gamma_{2'c}$ is very low compared with the theoretical results of others. Our L_{1c} transition is also low, but it compares better with the others than it does with Herman.

B. Hydrostatic Pressure

To calculate the effects of hydrostatic pressure on the band energies, we iterated to self-consistency using lattice constants of 5.42 and 5.442 Å, in addition to the equilibrium lattice constant of 5.431 Å. The results are presented in Table IV. The two sets of energy differences give one a feeling for the accuracy involved in taking small differences of quantities from different sets of iterations. The deformation energies are defined as

$$\text{D.E.} = -\frac{\delta E}{\delta V/V} = -\frac{\delta E}{(3\delta a/a)}$$

[25] M. Cardona, K. L. Shaklee, and F. H. Pollak, Phys. Rev. 154, 696 (1967).

[26] J. C. Phillips, Solid State Phys. 18, 55 (1966).

TABLE IV. Self-consistent energy eigenvalues for Si based on six-point zone sampling, Slater's exchange, 259 OPW's, and a lattice constant of 5.431 Å are given in column 2. The changes in the eigenvalues when self-consistency was obtained at 5.42 Å and 5.442 Å are given in columns 3 and 4. The resulting average deformation energies appear in column 5. Energies are in eV. Deformation energies are in eV per unit dilation.

Level	Energy (5.431 Å)	$E_{5.42}-E_{5.431}$	$E_{5.431}-E_{5.442}$	D.E.
Γ_{15c}	7.022	0.099	0.071	14.0
$\Gamma_{2'c}$	6.978	0.207	0.135	28.2
$\Gamma_{25'v}$	4.228	0.077	0.067	11.8
Γ_{1v}	−7.515	0.036	0.028	5.3
X_{1c}	5.512	0.054	0.059	9.3
X_{4v}	1.511	0.057	0.051	8.9
X_{1v}	−3.519	0.058	0.049	8.8
L_{3c}	8.059	0.077	0.068	11.9
L_{1c}	5.831	0.103	0.091	16.0
$L_{3'v}$	3.051	0.066	0.061	10.4
W_{2c}	9.059	0.067	0.078	11.9
W_{2v}	0.663	0.047	0.044	7.5
Δ_{1c}	5.781	0.070	0.064	11.0
Δ_{5v}	2.452	0.061	0.056	9.6
Σ_{3c}	7.109	0.086	0.078	13.5
Σ_{2v}	2.955	0.065	0.060	10.3

TABLE V. Comparison of theoretical and experimental net deformation energies for Si in eV per unit dilation. The ± indicates the difference from the average to the 5.42- and 5.442-Å results.

	Theory			
Transition	Present work	Goroff and Kleinman[a]	Herman[b]	Experiment
$L_{1c}-\Gamma_{25'v}$	−4.1±0.2	−4.1	−4.1	
$X_{1c}-\Gamma_{25'v}$	2.5±1.3	+0.3	+1.4	
$\Delta_{1c}{}^m-\Gamma_{25'v}$	+1.6±0.4		+1.4	+1.5[e] +3.71[d]
$\Delta_{1c}-\Gamma_{25'v}$	0.8±0.3		+0.7	
$\Gamma_{15c}-\Gamma_{25'v}$	−2.1±1.5	−1.35	−0.6	
$\Delta_{1c}-\Delta_{5v}$	−1.4±0.1		−1.3	
$X_{1c}-X_{4v}$	+0.9±0.4	−2.3	−1.4	
4.3-eV peak				−2.8±0.5[e]
$\Sigma_{3c}-\Sigma_{2v}$	−3.2±0.3		−3.1	
$\Gamma_{2'c}-\Gamma_{25'v}$	−16.3±5.1	−8.6	−11.9	
$L_{1c}-L_{3'v}$	−5.5±0.6	−4.5	−5.2	
3.4-eV peak				−5.0±0.5[e]
$L_{3c}-L_{3'v}$	−1.5±0.3		−1.1	

[a] Reference 27.
[b] Reference 8.
[e] Reference 28.
[d] Reference 29.
[e] References 30–33.

and are given in units of eV per unit dilation. a is the lattice constant.

Table V gives the physically more interesting deformation energy differences for Si. The ± gives the distance from the average to the separate column results of Table IV and is only a rough measure of the theoretical uncertainty. The theoretical values of Goroff and Kleinman[27] and Herman[8] are also presented together with the experimental results of Paul and Brooks,[28] Balslev,[29] Zallen,[30] and Gehardt.[31–33]

With a very few exceptions, our results agree within our limits of uncertainty with Herman's[8] results. A direct comparison with experiment can only be made on the $\Delta_{1c}{}^m-\Gamma_{25'v}$ deformation energy for the indirect band gap. Here we support Herman in our agreement with Paul and Brook's[28] value of 1.5 eV/unit dilation rather than with Balslev's[29] later value of 3.71 eV/unit dilation. The other experimental results give shifts of reflectivity peaks which involve contributions from large sections of the reduced zone.

C. Spin-Orbit Splitting

The spin-orbit splitting at Γ of the threefold degenerate $\Gamma_{25'v}$ was found from first-order perturbation theory on the self-consistent $\Gamma_{25'}$ valence wave functions to be 0.056 eV. Experimentally, the spin-orbit splitting has not been determined from an analysis of any doublet structure connected with the transition $\Gamma_{2'c}-\Gamma_{25'v}$. A precise value of the splitting 0.0441±0.004 eV has been

deduced by Zwerdling et al.,[34] from an analysis of the infrared spectrum of electronic transitions from the valence bands to acceptor impurity levels.

D. Effective Masses

Effective masses have been calculated for the top valence band at the Γ point and for the bottom of the conduction band at its minimum which occurs at 0.82 of the way along the Δ line between Γ and X. For the $\Gamma_{25'v}$ valence band (where spin-orbit splitting has been neglected) $m_\Gamma{}^*=0.8$ in the (1,1,1) direction and 0.3 in the (1,0,0) direction. Hensel, Hasegawa, and Nakayama[35] have measured the effective masses at the minimum in the conduction band. They obtained $m^*=0.1905$ and $m_{||}{}^*=0.9163$. The SCOPW effective mass at the minimum in the conduction band is $m_{||}{}^*=1.0$ in the (1,0,0) direction.

E. Density of States

In Figs. 4(a) and 4(b), the SCOPW density of states for the valence and conduction bands are given. The zero of energy for both the valence- and conduction-band density of states was taken at the top of the $\Gamma_{25'v}$ valence band. The location of the high-symmetry point bands is shown. It should be emphasized that these are merely the locations of high-symmetry point bands and do not imply that the given structure is due to the particular band.

In the valence-band density of states, the first broad peak below the top of the valence band is due to states near $L_{3'}, \Sigma_2, \Delta_5, X_4, \Sigma_1, \Delta_{2'},$ and W_2. The next peak down

[27] I. Goroff and L. Kleinman, Phys. Rev. 132, 1080 (1963).
[28] W. Paul and H. Brooks, Progr. Semicond. 7, 135 (1963).
[29] I. Balslev, Phys. Rev. 143, 636 (1966).
[30] R. Zallen, Gordon McKay Laboratory of Applied Science, Harvard University, report No. HP-12 (unpublished).
[31] U. Gerhardt, Phys. Letters 15, 401 (1965).
[32] U. Gerhardt, Phys. Status Solidi 11, 801 (1965).
[33] U. Gerhardt, Phys. Letters 9, 117 (1964).

[34] S. Zwerdling, K. J. Button, B. Lox, and L. M. Roth, Phys. Rev. Letters 4, 173 (1960).
[35] J. C. Hensel, H. Hasegawa, and M. Nakayama, Phys. Rev. 138, A225 (1965).
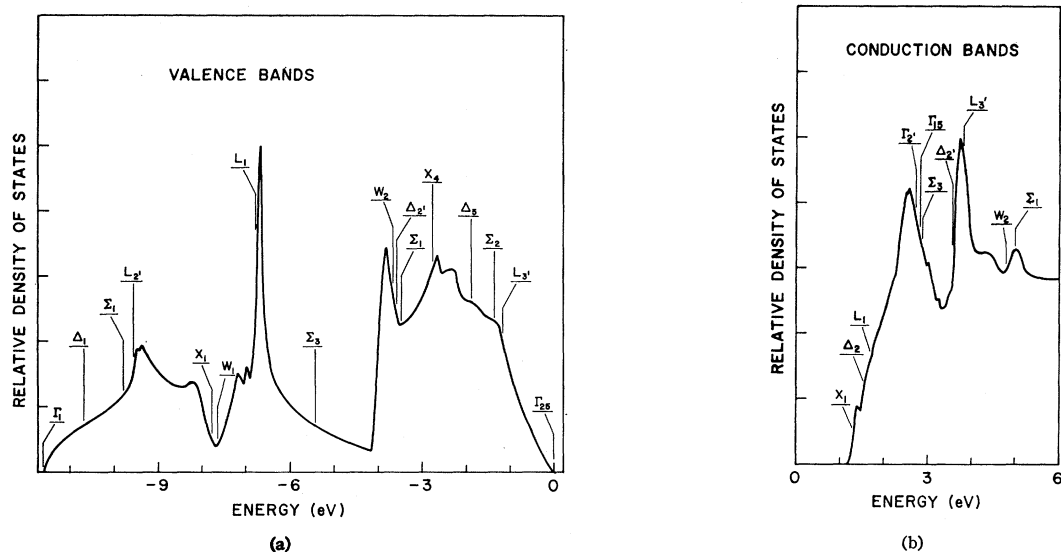
FIG. 4. (a) Electronic density of states for the valence bands of Si. (b) Electronic density of states for the conduction bands of Si.

originates in the flat area around L_1. The lowest peak is due to the s-like valence band. In the conduction-band density of states, the rapid rise to the first peak is due to the flat areas around L_1 and X_1. The second peak results primarily from the flat area around the $L_{3'}$.
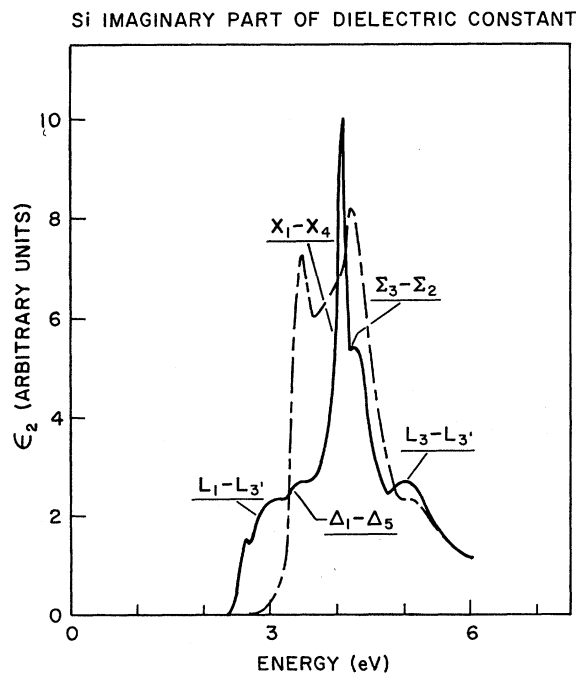
FIG. 5. Comparison of theoretical and experimental ϵ_2 curves for Si. The solid line gives the SCOPW ϵ_2 curve for Slater's exchange. The dashed line gives the experimental results of Phillipp and Ehrenreich.

F. Imaginary Part of Dielectric Constant

The imaginary part of the dielectric constant (ϵ_2) calculated from the bands obtained using the six-point zone sampling and Slater's exchange are shown in Fig. 5, together with the ϵ_2 calculated from experimental data by Phillipp and Ehrenreich.[36] Table VI gives a summary of the theoretical (present work and Brust's[1]) and experimental ϵ_2 peak positions.

We find that the interband transitions which are primarily responsible for the main reflectivity peak at 4.5 eV are from the outer part of the zone in the U-K region. This peak, which is commonly called $X_{1c}-X_{4v}$, came from a relatively large volume in the outer part of the zone. The broad weaker peak at about 5.3 eV is due to transitions closely related to the $L_{3c}-L_{3'v}$

TABLE VI. Comparison of theoretical and experimental peak positions for Si.

Peak	Theoretical ϵ_2 Present work	Brust[a]	Experimental Reflectivity	ϵ_2
$E_{0'}$		$\Gamma_{15c}-\Gamma_{25'v}$ 3.5	3.4[b]	
		$L_{1c}-L_{3'v}$ 3.15		
E_2	$X_{1c}-X_{4v}(U\text{-}K)$ regions 4.1	$X_{1c}-X_{4v}$ 4.0	4.5[c]	4.3[c]
	$L_{3'c}-L_{3v}$ region 5.0	$L_{3c}-L_{3'v}$ 5.2		5.3[d]

[a] Reference 1.
[b] Reference 32; B. O. Seraphin and W. Bottka, Phys. Rev. Letters 15, 104 (1965); B. O. Seraphin, Phys. Rev. 140, A1716 (1965).
[c] Reference 36; M. L. Cohen and J. C. Phillips, Phys. Rev. 139, A912 (1965).
[d] Reference 36.

[36] H. R. Phillipp and H. Ehrenreich, Phys. Rev. 129, 1550 (1963).

transition. It can be seen from Fig. 5 that for these two peaks our unadjusted theoretical peak positions match the experimental peak positions within a couple tenths of an eV. Brust and Kane have achieved similar results for these peaks, but, of course, they adjusted to do so.

It is clear from Fig. 5 that we have not been able to match the 3.4 eV peak—especially in intensity. We do have some structure at 3.4 eV which comes primarily from transitions near the $\Delta_{1c}-\Delta_{5v}$ transition. Phillips[37] has suggested that the difference between theory and experiment for the 3.4-eV peak (which has been found in all theoretical work) may be due to a strong exciton near 3.4 eV. Brust[1,38] and Kane[2] have been able to generate a 3.4-eV peak in their theoretical spectrum but it is not clear that their theoretical peak is, in fact, related to its experimental counterpart. Phillips,[26,39] Brust,[1,38] Cohen and Bergstresser,[3] Cardona and Pollak[4] and Kane[2] assign the 3.4-eV reflectivity peak so the $\Gamma_{15c}-\Gamma_{25'v}$ transition (or to closely related $\Delta_{1c}-\Delta_{5v}$ transitions). Of course, the $\Gamma_{15c}-\Gamma_{25'v}$ assignment is nominal since such a transition would give rise to an edge rather than a peak in the reflectivity spectrum.

G. Form Factors

Table II compares the experimental structure factors, corrected for thermal and anomalous dispersion, with the results of several different SCOPW calculations for Si. The theoretical procedures differ by the method used to approximate the exchange potential. The columns headed RHF (relativistic Hartree Fock) are obtained by placing relativistic Hartree-Fock free atoms in the crystal lattice. Those headed Sl contain results obtained using a Slater $\rho^{1/3}$ approximation, while KSG refers to the use of Kohn-Sham-Gaspar exchange. The symbol RHF added to any of these headings means that relativistic Hartree-Fock cores have been substituted for those obtained in the calculation. This is done because the main interest here lies in the valence contribution to the structure factors. From the study of gases, it is known that RHF results match experiment very closely.

[37] J. C. Phillips, Phys. Rev. Letters **10**, 329 (1963).
[38] D. Brust, Phys. Rev. **139**, A489 (1965).
[39] J. C. Phillips, Phys. Rev. **125**, 1931 (1962).

From our SCOPW experience, the iterated core changes little from the free atomic core. Consequently, the combination of the RHF core and the SCOPW valence structure factors give our best theoretical estimate. It It can be seen that KSG comes very close to RHF for the high-order reflections. In other words, these treatments of the exchange potential give a description of the core which is close to the true Hartree-Fock. One also sees that the experimental results depart from the free-atom RHF calculation for the 222 in Si. The departure, however, is in the opposite direction from that observed for metals, where the first Fourier components were lower than the RHF values, indicating a delocalization of the outer electrons. Here, on the contrary, they are higher, suggesting a localization of the valence electrons.

As can be seen, all of the exchange model results are in qualitative agreement with the experimental data. Thus, the band calculation does improve on the free-atom values. For the 111 reflection, it appears that the various exchange models used are not too satisfactory for Si. For the 222 reflection, all SCOPW calculations give excellent agreement with experiment and are improvements with respect to the RHF value.

IV. CONCLUSIONS

It should be emphasized that no adjustments are made in our SCOPW model. Input data consists of the crystal symmetry, the nuclear charge of Si, the lattice constant, and the exchange constant. The resulting agreement with experiment of such quantities as the energy and deformation energy of the indirect gap, the parallel effective mass of the conduction-band minimum, the $\Gamma_{25'v}$ spin-orbit splitting, and the ϵ_2 peak position is, thus, surprising, but is also consistent with past experience with this model. The mediocre agreement with experiment of the form factors, and the disagreement with all other theories of the $\Gamma_{2'c}$ energy must, however, be noted. We conclude that for Si, as for other tetrahedral semiconductors, the SCOPW model with Slater's exchange seems to work remarkably well. Apparently, for these tetrahedral crystals, Slater's exchange simulates the correct exchange plus correlation rather well, at least as far as energy eigenvalues are concerned.